Pressure dependence on the viscosities of 1-butyl-2,3-dimethylimidazolium bis(trifluoromethylsulfonyl)imide and two tris(pentafluoroethyl)trifluorophosphate based ionic liquids: new measurements and modeling

Félix M. Gaciño, Xavier Paredes, María J.P. Comuñas*, Josefa Fernández

Laboratorio de Propiedades Termofísicas, Departamento de Física Aplicada, Campus Vida, Universidad de Santiago de Compostela, E-15782 Santiago de Compostela, Spain

Corresponding author. *E-mail:* *mariajp.comunas@usc.es*

Tel.: +34 881814036; fax: +34 881814112.

ABSTRACT

New experimental viscosity data of three ionic liquids, 1-butyl-2,3-dimethylimidazolium tris(pentafluoroethyl)trifluorophosphate, 1-(2-methoxyethyl)-1-methyl-pyrrolidinium tris(pentafluoroethyl)trifluorophosphate and 1-butyl-2,3-dimethylimidazolium bis(trifluoromethylsulfonyl)imide, are reported in this work. The measurements were carried out using a falling-body viscometer in a temperature range from (313.15 to 363.15) K at pressures up to 150 MPa. These values were correlated as function of temperature and pressure with four different equations. Moreover, we perform an analysis of the dependency of viscosity on pressure and temperature based on the density scaling concept for these fluids and other three ionic liquids recently studied with the same device.

Keywords: Ionic liquids, Viscosity, High Pressures, Density Scaling.

1. Introduction

The thermophysical characterization of ionic liquids (ILs) is an important task that is currently being undertaken in order to determine their possible applications. Some of these potential uses lie in the fields of clean oilfield technologies, dye-sensitized solar cells, chemical and environmental engineering, polymer sciences, material chemistry, catalysis, nanotechnology, biotechnology or electrochemical applications [1-6]. ILs present many unique properties, such as negligible volatility, non-flammability, high thermal stability, high thermal conductivity, low melting point, low temperature fluidity and broad liquid range. These properties and the fact that their viscosity can be tailored make them an excellent alternative to substitute volatile organic solvents and conventional lubricants.

Their use as lubricants is one of the most researched applications during the last years. In 2001 Ye et al. [7] reported tribological tests for alkylimidazolium tetrafluoroborate salts. These fluids showed excellent friction reduction, antiwear performance and high load-carrying capacity for different types of contact pairs like steel/steel, steel/aluminium, steel/copper, steel/SiO_2, Si_3N_4/SiO_2, steel/Si(100), steel/sialon ceramics and Si_3N_4/sialon ceramics. Since then, the number of articles concerning their use as lubricants or lubricant additives has increased significantly and currently there are more than 240 articles published [8-14]. The high polarity of the ILs makes them capable of forming very strong effective adsorption films and ready tribochemical reactions, which contributes to their prominent antiwear capability [10].

To develop a new kind of lubricant for gears it is required an analysis of the behavior of the viscosity as a function of the pressure and the temperature [15-17] in order to ensure that the oil is in elastohydrodynamic regime during operation at the gear conditions. One of the most interesting characteristics of the ILs is that many of their

physical and chemical properties, among them the viscosity, can be modified by selecting different lengths of the nonpolar alkyl chain of the cations or different types of anions [18] in order to suit an application. The most researched ILs in lubrication [14, 19] are based on imidazolium, pyridinium, phosphonium or ammonium cations and the anions tetrafluoroborate $[BF_4]^-$, hexafluorophosphate $[PF_6]^-$, bis(trifluoromethylsulfonyl)imide $[NTf_2]^-$, bis(perfluoroethylsulfonyl)imide $[(C_2F_5SO_2)_2N]^-$, tris(pentafluoroethyl)tri-fluorophosphate $[(C_2F_5)_3PF_3]^-$ and trifluoromethanesulfonate $[CF_3SO_3]^-$. Nevertheless, ILs with $[BF_4]^-$ and $[PF_6]^-$ are nowadays avoided because they react with water producing hydrofluoric acid (HF) [20, 21].

The viscosity at atmospheric pressure is currently one of the most studied properties for these fluids [19]. Contrarily, studies on the viscosity-pressure behavior of ILs are quite scarce, although new articles on this subject are rising [22-26]. Our research group is characterizing some thermodynamic properties of ILs, such as the density and viscosity at atmospheric pressure [18] and at high pressures [22, 27].

In this work, we provide the viscosities from (313.15 to 363.15) K at pressures up to 150 MPa of three ILs: 1-butyl-2,3-dimethylimidazolium tris(pentafluoroethyl)-trifluorophosphate $[C_4C_1C_1Im][(C_2F_5)_3PF_3]$, 1-(2-methoxyethyl)-1-methylpyrrolidinium tris(pentafluoroethyl)trifluorophosphate $[C_1OC_2C_1Pyrr][(C_2F_5)_3PF_3]$, and 1-butyl-2,3-dimethylimidazolium bis(trifluoromethylsulfonyl)imide $[C_4C_1C_1Im][NTf_2]$. The measurements were carried out using a falling body viscometer VisLPT1 that has been recently implemented in our laboratory [22]. We also provide correlations of the experimental viscosity values as function of temperature and pressure with four equations and an analysis of the results using the “thermodynamic” or “power law density” scaling [28-33].

2. Experimental Section

2.1 Materials

The samples of analyzed ILs were kindly provided by Merck KGaA with mole fraction purity higher than 98%. The manufacturer gives the mole-fraction higher than 99.0% for $[C_1OC_2C_1Pyrr][(C_2F_5)_3PF_3]$ determined by electrophoresis and 99.9% for $[C_4C_1C_1Im][NTf_2]$ determined by high-performance liquid chromatography. The molecular structures of the three liquids are summarized in table 1.

To remove traces of water and volatile compounds, IL samples were dried under constant stirring and at moderate vacuum (8 Pa) for several days. The water content of each IL was determined by Karl Fischer titration using a Mettler Toledo DL32 coulometer. The reagent used was Hydranal - Coulomat AG from Fluka. The water content of each IL is reported in table 1. To avoid the adsorption of moisture, the IL samples were transferred to the viscometer using a glass syringe through a Hamilton valve, HV Standard PTFE.

2.2 High pressure viscometer

Viscosities of the ILs were measured with a falling body viscometer (VisLPT1) which can operate at pressures up to 150 MPa. This equipment has been described previously [22]. The hemispherical sinker employed in this work is made of magnetic steel and it has a diameter of 6.10 mm, a length of 20 mm and a density of ρ_s = 7.695 $g \cdot cm^{-3}$. The temperature is regulated with a Lauda Proline RP 1840 thermostat and measured with a thermocouple located in the inner tube which is in contact with the sample. The pressure is measured with a transducer HBM P3MB and a numeric indicator HBM Scout 55. The accuracy of the thermocouple and the transducer are ± 0.5

K and ± 0.2 MPa, respectively. The measuring principle of this device is based on the relationship between the time (Δt) that a solid takes to fall inside the inner tube, once it has reached its terminal velocity under conditions of laminar flow, through a viscous fluid, and its viscosity (η) [34]. The assumption of laminar flow implies that the Reynolds number, R_e, has to be low. To estimate R_e, we have taken into account three different criteria proposed by Isdale et al. [29], by Chen et al. [30] and by Lohrenz and Kurata [31]. Following the same procedure that we have performed in a previous work [22], we have checked that the performed measurements were carried out under laminar flow. As an example, in figure 1 we plot the results obtained for the three ILs following the Isdale et al. criteria [29].

The working equation used to estimate the viscosity is as follows [22, 35, 36]:

$$\eta = a + b \cdot (\Delta\rho \cdot \Delta t) + c \cdot (\Delta\rho \cdot \Delta t)^2 \quad (1)$$

where a, b and c are the calibration parameters, and $\Delta\rho = \rho_S - \rho_L$ is the difference between the densities of the sinker and the liquid under study, respectively. The calibration parameters have been obtained by using diisodecyl phthalate and bis(2-ethylhexyl) phthalate as in our previous work [22]. Squalane has been used to verify the calibration procedure. Taking into account the precision in pressure, temperature, falling time and reference viscosity values of diisodecyl phthalate and bis(2-ethylhexyl) phthalate used to perform the calibration, we have estimated a viscosity uncertainty of 5%. The biggest contribution to the viscosity uncertainty is due to the temperature measurement.

As it is can be observed in equation (1), calculation of the viscosity from fall times requires knowledge of the density as a function of temperature and pressure. For this purpose, the Tammann-Tait density correlations for the three ILs, previously published by our research group [37], were used. These correlations have been obtained

from experimental densities measured by using a vibrating tube densimeter Anton Paar DMA HPM in a temperature range (278.15 to 398.15) K and at pressure up to 120 MPa.

3. Results and discussion

In this work the falling times, Δt, for three ILs have been measured with the described device. The data have been acquired up to 150 MPa at three temperatures ranging from (313.15 to 363.15) K for $[C_1OC_2C_1Pyrr][(C_2F_5)_3PF_3]$, and $[C_4C_1C_1Im][NTf_2]$, and at two isotherms (313.15 K and 343.15 K) for $[C_4C_1C_1Im][(C_2F_5)_3PF_3]$. In table 2 the viscosities are presented whereas in figure 2 we have plotted the experimental values of the three ILs at 313.15 K as a function of the pressure. In figure 3 viscosity values for $[C_4C_1C_1Im][NTf_2]$ are plotted, as an example of the viscosity behavior with the pressure and the temperature. As far as we know, there are no available reported data at high pressures for the studied ILs.

The viscosities of the ILs as function of temperature and pressure were correlated with three different modified Vogel-Fulcher-Tammann (VFT) equations (equations (2)-(4)) and with a modified Litovitz equation (equation (5)). These equations are as follows:

$$\eta(p,T) = A \cdot exp\left(B/(T-C)\right)\left(\left(p+E(T)\right)/\left(p_{ref}+E(T)\right)\right)^D \quad (2)$$

where A, B and C are obtained fitting viscosity data at the reference pressure (0.1 MPa) as a function of temperature, and E(T) is a second-degree polynomial

$$E(T) = E_0 + E_1 \cdot T + E_2 \cdot T^2$$

$$\eta(p,T) = exp\left(a + bp + \left(c + dp + ep^2\right)/(T - T_0)\right) \quad (3)$$

$$\eta(p,T) = exp\left(a + bp + cT_0(p)/(T - T_0(p))\right) \quad (4)$$

where: $T_0(p) = d + e \cdot p + f \cdot p^2$

$$\eta(p,T) = exp\left(a + bp + \left(c + dp + ep^2\right)/T^3\right) \quad (5)$$

Equation (2) was proposed by Comuñas et al [38], whereas equations (3)-(5) were used by Harris et al. [23]. To perform these correlations we have used together with the data reported in table 2, the viscosities at atmospheric pressure that we have previously measured in a rotational viscometer Anton Paar Stabinger SVM3000 [18] from 283.15 to 373.15 K for $[C_4C_1C_1Im][(C_2F_5)_3PF_3]$, from 258.15 K to 373.15 K for $[C_1OC_2C_1Pyrr][(C_2F_5)_3PF_3]$ and from 273.15 K to 373.15 K for $[C_4C_1C_1Im][NTf_2]$.

The values of the parameters of equations (2)-(5) are gathered in table 3. The modified VFT equations lead to good correlations of the experimental values, especially with equation 2, which provides an AAD lower than 2.0 % for the three ILs. On the other hand, the modified Litovitz equation (equation (5)) gives the largest deviations, especially for $[C_1OC_2C_1Pyrr][(C_2F_5)_3PF_3]$ for which a maximum deviation of 14.4 % is obtained.

In previous works [14, 18, 22] we have analyzed the viscosity trend of several ILs as a function of the molecular structure. Regarding the effect of the cation structure, in the analyzed temperature range and at atmospheric pressure the viscosity trend found for $[NTf_2]^-$ based ILs is: $[C_{10}C_1Im]^+ \approx [C_4C_1C_1Im]^+ > [C_6C_1Im]^+ > [C_4C_1Im]^+ > [C_2C_1Im]^+$, i.e. the viscosity increases as the length or the number of carbon atoms of alkyl chains of the imidazolium cation [18] increases. These trends are kept as the pressure increases, as it can be observed in figure 4 at 313.15 K. Harris et al. [24] have measured the viscosity of the $[C_4C_1Im][NTf_2]$ in a temperature range of (273.15 and 353.15) K and at maximum pressures of 300 MPa. By comparison of their data with the experimental results obtained in this work for $[C_4C_1C_1Im][NTf_2]$, we observe that the addition of another methyl group on the $[C_4C_1Im]^+$ cation leads to a viscosity increase of up to 75 %. This result agrees with previous findings by Fumino et al. [39, 40] for

$[C_2C_1C_1Im][NTf_2]$ and $[C_2C_1Im][NTf_2]$ and by Hunt et al. [41] for $[C_4C_1C_1Im][Cl]$ and $[C_4C_1Im][Cl]$. Fumino et al. [39, 40] have showed that adding a methyl branch to the C2 position of the cation, a strong, localized and highly directional H bond is replaced by a long range Coulomb interaction, symmetrizing the charge network (making it more ionic-like). With a more regular and tight packed structure, it can be observed an increase in viscosity and melting point [42]. Concerning the effect of the anion structure it was concluded in previous works [14, 18, 22], that for ILs based on different cations, $[NTf_2]^-$ ILs are less viscous than $[(C_2F_5)_3PF_3]^-$ ILs. In this work we have verified that the same behavior is kept for $[C_4C_1C_1Im]^+$ ILs at broad temperature and pressure conditions (figure 2).

The local pressure–viscosity coefficient, $\alpha(p)$, is an important parameter to characterize the suitability of a lubricant [22], which has been determined to characterize the viscosity-pressure dependence at a fixed temperature. The equation employed to calculate this parameter is as follows:

$$\alpha(p) = \frac{1}{\eta}\left(\frac{\partial \eta}{\partial p}\right)_T \tag{6}$$

The $\alpha(p)$ values were obtained by using this equation together equation (2) for the three ILs reported in this work (table 4). The pressure-viscosity coefficients for $[C_4C_1C_1Im][(C_2F_5)_3PF_3]$ are almost pressure independent. The $\alpha(p)$ behavior as a function of pressure and temperature is plotted for the IL $[C_1OC_2C_1Pyrr][(C_2F_5)_3PF_3]$ in figure 5. The local pressure–viscosity coefficient decreases with temperature and slightly with pressure for this IL. Figure 6 shows that the two ILs based on the $[(C_2F_5)_3PF_3]^-$ anion present $\alpha(p)$ values quite higher than those of ILs based in the $[NTf_2]^-$ anion. In figure 7 we compare the $\alpha(p)$ behavior of both $[(C_2F_5)_3PF_3]^-$ ILs with those of squalane, two poly(propylene oxide) dimethyl ethers (PAG2 and PAG3) and

two dipentaerythritol esters. Squalane can be considered a mineral-lubricant model, the polypropylene glycol dimethyl ethers and the polyesters are synthetic base oils [43-47]. The thickness of the oil film in gears depends on the pressure viscosity coefficients. The higher the α value, the thicker the film in the gear contact. Figure 7 shows that the $[(C_2F_5)_3PF_3]^-$ ILs present $\alpha(p)$ values higher than those of dipentaerythritol esters and similar to those of PAG2 and PAG3. Because of mineral oils are the lubricants with the highest $\alpha(p)$ values, it is noticeable that at pressures higher than 120 MPa both ILs have higher $\alpha(p)$ values than squalane. This means that these ILs can avoid boundary wear at high loads.

In order to provide a more general framework describing the dependency of the viscosity on density and temperature, the "thermodynamic" or "power law density" scaling is examined for several ILs. Many authors have reported [28, 31, 48-51] that several dynamic properties can be expressed as functions of the temperature, T, and volume, V, through a scaling relation as follows:

$$x(T,V) = \psi\left(TV^{\gamma}\right) \tag{7}$$

where x is the dynamic property and γ is an empirically determined constant characteristic of the fluid. This scaling relation has been obtained for the dielectric relaxation time, τ, the viscosity, η, the self-diffusion coefficients, D, and the electrical conductivities, κ. The γ constant reflects the repulsive intermolecular force, although for complex molecules or ions it can also include contributions from internal molecular modes, such as vibrations and torsions, and be affected by the attractive intermolecular forces [52].

Pensado et al. [29] have proposed an expression for the function ψ for viscosities. This expression is based on a work of Casalini and Roland [48] on relaxation times, and presents the following form:

$$\eta(T,V) = \eta_0 \exp\left[\left(A/TV^{\gamma}\right)\right]^{\phi} \quad (8)$$

The parameters η_0, A, γ, ϕ of equation (8) can be obtained by fitting the viscosity data at different temperatures and volumes. Hereafter, we have obtained their values for the three ILs studied in this work and for other ILs that had been studied in a previous work [22]. These liquids are 1-(2-methoxyethyl)-1-methylpyrrolidinium bis(trifluoromethylsulfonyl)imide, $[C_1OC_2C_1Pyrr][NTf_2]$; 1-butyl-1-methylpyrrolidinium bis(trifloromethylsulfonyl)imide, $[C_4C_1Pyrr][NTf_2]$; and 1-ethyl-3-methylimidazolium ethylsulfate, $[C_2C_1Im][C_2SO_4]$. In order to assess equation (8) graphically, we plot in figure 8 the experimental viscosities of the six ILs as a function of $\rho^{\gamma}\cdot T^{-1}$, where it can be observed that the experimental data of each IL fall within a unique curve.

In table 5 we present the values obtained for the characteristic parameters of equation (8). Harris et al. [23] have also fitted their experimental viscosity data of $[C_4C_1Pyrr][NTf_2]$ to equation (8). Comparing their values of γ and ϕ, they are similar to our reported values: for γ they have obtained a value of 3.06 versus the 3.16 value obtained in this work for the same IL, whereas concerning to the ϕ parameter, they have reported a value of 2.16 versus our 2.36 value.

As can be seen in table 5, our γ values range from 2.69 to 4.29, whereas ϕ parameter ranges from 2.34 to 3.17. López et al. [52] have fitted equation (8) for 11 ILs and 35 molecular compounds. The γ values obtained by these authors varies from 1.76 for methanol and 13.54 for cyclopentane, whereas the γ range for the ILs is narrow, varying from 2.18 for $[C_8C_1Im][BF_4]$ to 3.54 for $[C_1C_1Im][C_1SO_4]$. The γ values of the ILs studied here fall in this last range except for both ILs with $[(C_2F_5)_3PF_3]^-$ anion with γ values of 3.74 and 4.29, which are similar to those of synthetic oils like squalane, pentaerythritol tetra-2-ethylhexanoate and pentaerythritol tetranonanoate [29]. The

lower is the γ, the stronger are the molecular interactions [28, 52] and/or the number of molecule bonds. Hence, $[(C_2F_5)_3PF_3]^-$ anion does not lead to strong interactions in comparison with the other ILs of table 5 and those studied by López et al. which are based in $[BF_4]^-$, $[PF_6]^-$, $[NTf_2]^-$, $[C_1SO_4]^-$, $[B(C_4H_9)_4]^-$ and tosylate anions. These means that the role of the temperature in the transport properties (diffusion, electrical conductivity and viscosity) is less important in $[(C_2F_5)_3PF_3]^-$ ILs. Comparing the γ values for all the ILs based in the $[NTf_2]^-$ anion, we have obtained the following increasing trend with the cation $[C_6C_1Im]^- < [C_4C_1C_1Im]^- < [C_4C_1Im]^- < [C_4C_1Pyrr]^- < [C_1OC_2C_1Pyrr]^-$. Further studies are needed to verify if this trend is kept for ILs based in other anions.

Fragiadakis and Roland [53] have proposed writing the transport properties in reduced forms when superposition curves are performed. The reduced form for the viscosity is as follows:

$$\eta^* = v^{2/3}\left(mk_BT\right)^{-1/2}\eta \tag{9}$$

where m is the molecular mass and v the liquid volume per molecule (v=V/N, being N the total number of molecules in a liquid volume V). According to these authors only the scaling coefficient obtained using reduced quantities (γ^*) can be sensibly related to the intermolecular potential [53]. This new scaling exponent γ^* presents lower values than γ because as the viscosity decreases with the temperature, the product $\eta T^{-1/2}$ decreases still stronger, so the effect of temperature on the reduced viscosities is stronger than on the actual viscosities [52, 53]. The factor $v^{2/3}$ almost does not affect the γ^* values.

According to the results published by López et al. [52], both scaling exponents, γ and γ^*, present significant differences for molecular liquids as n-hexane, ammonia or cyclopentane among others, but for the six ionic liquids studied by these authors these

differences between γ and γ^* are almost negligible, obtaining the maximum deviation for $[C_4C_1Im][NTf_2]$ with γ=2.89 and γ^*=2.70.

The scaling exponent γ^* was determined for the six ILs of table 5 using the equation (8) in a similar way that for the unreduced viscosity. Thus, applying equation (8) with the reduced viscosity through equation (9) we obtained the reduced parameters (η_0^*, A^*, γ^*, ϕ^*) gathered in table 5. In figure 9 we have plotted the reduced viscosity for $[C_1OC_2C_1Pyrr][NTf_2]$ as function of density and as function of $1000\rho^{\gamma^*}\cdot T^{-1}$, the behavior being similar to that obtained using non reduced viscosity. Comparing the scaling exponents, the values of the reduced scaling exponent, γ^*, are slightly lower than γ in agreement with the results of López et al. [52] for other ILs. Both parameters present the same trend with the molecular structure of the ions.

From these scaling exponents, we can try to clarify the intermolecular interactions that affect the ILs. As it was concluded by Roland et al. for other ILs [28], the small values of γ and γ^* reflect the weak contribution of the volume to the dynamics of these liquids. So that, the dynamics primarily reflect the influence of temperature and it seems to be consistent with a strong intermolecular force due to the electrostatic interaction. However, according to the values obtained, the ILs containing the $[(C_2F_5)_3PF_3]^-$ anion seem to be mainly affected by van der Waals interactions, corresponding to bulkier anions.

4. Conclusions

New viscosity data at high pressures are reported for three ILs for which no experimental viscosities were previously published. The correlations for these values together with those at 0.1 MPa to VFT-modified equations were successful, but the correlation to the Litovitz equation presents higher deviations. The effect of the cation

and the anion on the viscosity follow this sequence: for the cation we have found $[C_{10}C_1Im]^+ \approx [C_4C_1C_1Im]^+ > > [C_6C_1Im]^+ > [C_4C_1Im]^+ > [C_2C_1Im]^+$, whereas for the anion $[(C_2F_5)_3PF_3]^- > [NTf_2]^-$.

The scaling exponent obtained for the viscosity of six ILs ranges from 2.69 to 4.29, and the value obtained for $[C_1OC_2C_1Pyrr][(C_2F_5)_3PF_3]$ is similar to other synthetic oils as squalane, pentaerythritol tetra-2-ethylhexanoate and pentaerythritol tetranonanoate. For the reduced viscosity similar values of the scaling exponent were obtained. From the values obtained we identify the temperature as the main contribution to the dynamics of these liquids. It seems to be consistent with a strong intermolecular force due to the electrostatic interaction, although ILs containing the $[(C_2F_5)_3PF_3]^-$ anion seem to be mainly affected by van der Waals interactions.

Acknowledgments

Authors acknowledge Merck KGaA for the samples provided. We thank technical engineer Mr. Thierry Mesplou-Candau from the Groupe de Hautes Pressions of the University of Pau for the design of the detection circuit for the falling time. This work was supported by Spanish Ministry of Science and Innovation and EU FEDER Program through CTQ2008-06498-C02-01 and CTQ2011-23925 projects.

References

[1] R. Martínez-Palou, P. Flores Sánchez, in: Ionic Liquids: Theory, Properties, New Approaches, InTech, 2011, pp. 567-630.
[2] C.-P. Lee, P.-Y. Chen, K.-C. Ho, in: Ionic Liquids: Theory, Properties, New Approaches, InTech, 2011, pp. 631-656.
[3] A. Stojanovic, C. Morgenbesser, D. Kogelnig, R. Krachler, B.K. Keppler, in: Ionic Liquids: Theory, Properties, New Approaches, InTech, 2011, pp. 657-680.
[4] J. Lu, F. Yan, J. Texter, Prog. Polym. Sci. 34 (2009) 431-448.
[5] E. Aguilera-Herrador, R. Lucena, S. Cárdenas, M. Valcarcel, in: Ionic Liquids: Applications and Perspectives, 2011, pp. 181-206.
[6] A. Kokorin, Ionic Liquids: Applications and Perspectives, InTech, Rijeka, Croatia, 2011.
[7] C. Ye, W. Liu, Y. Chen, L. Yu, Chem. Commun. (2001) 2244-2245.
[8] I. Minami, Molecules 14 (2009) 2286-2305.
[9] M.-D. Bermúdez, A.-E. Jiménez, J. Sanes, F.-J. Carrión, Molecules 14 (2009) 2888-2908.
[10] F. Zhou, Y. Liang, W. Liu, Chem. Soc. Rev. 38 (2009) 2590-2599.
[11] M. Uerdingen, in: Handbook of Green Chemistry, Wiley-VCH Verlag GmbH & Co. KGaA, 2010.
[12] P. Wasserscheid, R.v. Hal, A. Bosmann, Green Chem. 4 (2002) 400-404.
[13] M. Palacio, B. Bhushan, Tribol. Lett. 40 (2010) 247-268.
[14] A.S. Pensado, M.J.P. Comuñas, J. Fernández, Tribol. Lett. 31 (2008) 107-118.
[15] H. Arora, P.M. Cann, Tribol. Int. 43 (2010) 1908-1916.
[16] A. Somers, P. Howlett, J. Sun, D. MacFarlane, M. Forsyth, Tribol. Lett. 40 (2010) 279-284.
[17] X. Paredes, O. Fandiño, A.S. Pensado, M.J.P. Comuñas, J. Fernández, Tribol. Lett. 45 (2012) 89-100.
[18] F.M. Gaciño, T. Regueira, L. Lugo, M.J.P. Comuñas, J. Fernández, J. Chem. Eng. Data 56 (2011) 4984-4999.
[19] S. Aparicio, M. Atilhan, F. Karadas, Ind. Eng. Chem. Res. 49 (2010) 9580-9595.
[20] M.G. Freire, C.M.S.S. Neves, I.M. Marrucho, J.A.P. Coutinho, A.M. Fernandes, J. Phys. Chem. A 114 (2009) 3744-3749.
[21] S.P.M. Ventura, R.L. Gardas, F. Gonçalves, J.A.P. Coutinho, J. Chem. Techol. Biot. 86 (2011) 957-963.
[22] F.M. Gaciño, X. Paredes, M.J.P. Comuñas, J. Fernández, J. Chem. Thermodyn. 54 (2012) 302–309.
[23] K.R. Harris, L.A. Woolf, M. Kanakubo, T. Rüther, J. Chem. Eng. Data 56 (2011) 4672–4685.
[24] K.R. Harris, M. Kanakubo, L.A. Woolf, J. Chem. Eng. Data 52 (2007) 1080-1085.
[25] K.R. Harris, M. Kanakubo, L.A. Woolf, J. Chem. Eng. Data 52 (2007) 2425-2430.
[26] I. Bandrés, R. Alcalde, C. Lafuente, M. Atilhan, S. Aparicio, J. Phys. Chem. B 115 (2011) 12499-12513.
[27] T. Regueira, L. Lugo, J. Fernández, J. Chem. Termodyn. 48 (2012) 213–220.
[28] C.M. Roland, S. Bair, R. Casalini, J. Chem. Phys. 125 (2006) 124508.
[29] A.S. Pensado, A.A.H. Padua, M.J.P. Comunas, J. Fernandez, J. Phys. Chem. B 112 (2008) 5563-5574.
[30] A. Grzybowski, K. Koperwas, M. Paluch, Phys. Rev. E 86 (2012) 031501.

[31] S. Bair, A. Laesecke, J. Tribol. 134 (2012) 021801.
[32] E.R. López, A.S. Pensado, J. Fernández, K.R. Harris, J. Chem. Phys. 136 (2012) 214502.
[33] G. Galliero, C. Boned, J. Fernández, J. Chem. Phys. 134 (2011) 064505.
[34] J. Kestin, W.A. Wakeham, Transport properties of fluids: Thermal conductivity, viscosity and diffusion coefficient, Purdue Research Foundation, New York, 1988.
[35] P. Daugé, A. Baylaucq, L. Marlin, C. Boned, J. Chem. Eng. Data 46 (2001) 823-830.
[36] M.J.P. Comuñas, A. Baylaucq, C. Boned, J. Fernández, Ind. Eng. Chem. Res. 43 (2004) 804-814.
[37] J. Fernández, J. Salgado, X. Paredes, T. Regueira, F.M. Gaciño, I. Otero, Ionic liquids as gear lubricants and hydraulic fluids, in: International Workshop on Ionic Liquids– Seeds for New Engineering Applications, Lisbon, Portugal, 2012.
[38] M.J.P. Comuñas, A. Baylaucq, C. Boned, J. Fernández, Int. J. Thermophys. 22 (2001) 749-768.
[39] K. Fumino, A. Wulf, R. Ludwig, Angew. Chem. Int. Ed. 47 (2008) 3830-3834.
[40] K. Fumino, A. Wulf, R. Ludwig, Angew. Chem. Int. Ed. 47 (2008) 8731-8734.
[41] P.A. Hunt, J. Phys. Chem. B 111 (2007) 4844-4853.
[42] K. Noack, P.S. Schulz, N. Paape, J. Kiefer, P. Wasserscheid, A. Leipertz, Phys. Chem. Chem. Phys. 12 (2010) 14153-14161.
[43] X. Paredes, A.S. Pensado, M.J.P. Comuñas, J. Fernández, J. Chem. Eng. Data 55 (2010) 3216-3223.
[44] X. Paredes, A.S. Pensado, M.J.P. Comuñas, J. Fernández, J. Chem. Eng. Data 55 (2010) 4088-4094.
[45] X. Paredes, O. Fandiño, A.S. Pensado, M.J.P. Comuñas, J. Fernández, Tribol. Lett. 45 (2012) 89-100.
[46] L.R. Rudnick, S.Z. Erhan, in: Synthetics, Mineral Oils, and Bio-Based Lubricants, CRC Press, Boca Raton, 2006.
[47] M.J.P. Comuñas, X. Paredes, F. Gaciño, J. Fernández, J.P. Bazile, G. Galliero, C. Boned, J. Pauly, J.L. Daridon, K.R. Harris, J. Phys. Chem. Ref. Data, to be submitted (2012).
[48] R. Casalini, C.M. Roland, J. Non-Cryst. Solids 353 (2007) 3936-3939.
[49] R. Casalini, C.M. Roland, Phys.Rev. E 69 (2004) 062501.
[50] C. Alba-Simionesco, A. Cailliaux, A. Alegría, G. Tarjus, Europhys. Lett. 68 (2004) 58.
[51] C. Dreyfus, A.L. Grand, J. Gapinski, W. Steffen, A. Patkowski, Eur. Phys. J. B 42 (2004) 309-319.
[52] E.R. López, A.S. Pensado, M.J.P. Comuñas, A.A.H. Padua, J. Fernández, K.R. Harris, J. Chem. Phys. 134 (2011) 144507.
[53] D. Fragiadakis, C.M. Roland, J. Chem. Phys. 134 (2011) 044504.
[54] J.D. Isdale, J.H. Dymond, T.A. Brawn, High Temp. High Press. 11 (1979) 571-580.
[55] A. Ahosseini, A. Scurto, Int. J. Thermophys. 29 (2008) 1222-1243.

TABLE 1

Ionic liquids studied in this paper

Chemical Formula CAS Number	Water content ppm	Chemical structures: Cation	 Anion	Name	Supplier	Mole fraction purity
$[C_4C_1C_1Im][(C_2F_5)_3PF_3]$	28	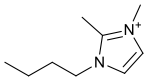	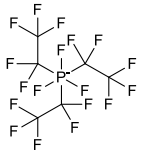	1-butyl-2,3-dimethylimidazolium tris(pentafluoroethyl) trifluorophosphate	Merck KGaA	>98%
$[C_1OC_2C_1Pyrr][(C_2F_5)_3PF_3]$ 1195983-48-2	7	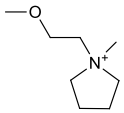	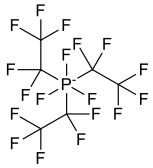	1-(2-Methoxyethyl)-1-methyl-pyrrolidinium tris(pentafluoroethyl) trifluorophosphate	Merck KGaA	>99%
$[C_4C_1C_1Im][NTf_2]$ 350493-08-2	16	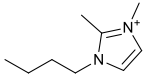	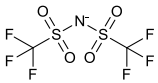	1-butyl-2,3-dimethylimidazolium bis(trifluoromethylsulfonyl) imide	Merck KGaA	>99.9%

TABLE 2

Viscosity values of the ILs studied in this work

T/K	p/MPa	η / mPa.s		
		$[C_1OC_2C_1Pyrr][(C_2F_5)_3PF_3]$	$[C_4C_1C_1Im][(C_2F_5)_3PF_3]$	$[C_4C_1C_1Im][NTf_2]$
313.15	10	64.0	81.1	55.9
313.15	15	69.9	88.9	59.5
313.15	25	83.0	106.8	67.3
313.15	50	126.1	167.4	90.7
313.15	75	189.7	260.6	120.9
313.15	100	283.3	403.5	159.8
313.15	125	421.1	622.7	210.1
313.15	150	623.8	958.7	275.0
343.15	10	22.6	25.3	19.5
343.15	15	24.2	27.2	20.5
343.15	25	27.7	31.2	22.7
343.15	50	38.6	44.1	28.8
343.15	75	53.4	62.0	36.3
343.15	100	73.8	87.3	45.5
343.15	125	102.2	123.5	56.9
343.15	150	142.5	176.1	70.9
363.15	10	14.8	-	12.4
363.15	15	15.8	-	13.0
363.15	25	18.1	-	14.3
363.15	50	24.5	-	17.9
363.15	75	32.3	-	22.1
363.15	100	41.7	-	26.9
363.15	125	53.2	-	32.4
363.15	150	66.9	-	38.7

Standard uncertainties are u(T) = 0.5 K, u(p) = 0.2 MPa and u(η) = 5%.

TABLE 3
Parameters of the correlation equations

	$[C_1OC_2C_1Pyrr][(C_2F_5)_3PF_3]$	$[C_4C_1C_1Im][(C_2F_5)_3PF_3]$	$[C_4C_1C_1Im][NTf_2]$
		Equation (2)	
A / mPa·s	0.15466	0.15612	0.1426
B / K	840.84	790.23	829.77
C / K	170.65	183.54	171.95
D	17.301	730.3	9.635
E_0 / MPa	-8705.6	-26973	-12095
E_1 / MPa	51.58	76.017	72.425
$10^2 \cdot E_2$ / MPa	-0.065548	0.45582	-0.09988
AAD / %	1.9	0.3	1.0
Bias / %	0.1	-0.1	0.0
MaxD / %	8.5	1.9	4.0
		Equation (3)	
a	-1.6139	-1.8169	-1.7337
$10^3 \cdot b$ / MPa^{-1}	-0.62429	-2.2842	0.63269
c / K	776.89	779.06	772.02
d / K·MPa^{-1}	2.4188	2.5653	1.5696
$10^5 \cdot e$ / K·MPa^{-2}	-94.888	-6.3395	-86.029
T_0 / K	175.3	184.43	176.53
AAD / %	2.3	0.3	1.6
Bias / %	-0.1	0.0	0.0
MaxD / %	7.2	1.7	4.1
		Equation (4)	
a	-1.6185	-1.8341	-1.7313
$10^3 \cdot b$ / MPa^{-1}	4.912	5.0147	4.044
c	4.4458	4.2554	4.3718
d / K	175.14	184.1	176.53
$10^2 \cdot e$ / K·MPa^{-1}	15.906	15.469	10.819
$10^5 \cdot f$ / K·MPa^{-2}	-19.571	-14.615	-13.335
AAD / %	2.1	0.3	1.5
Bias / %	-0.1	0.0	0.0
MaxD / %	7.1	1.5	4.1
		Equation (5)	
a	-0.3823	-0.61649	-0.4546
$10^3 \cdot b$ / MPa^{-1}	5.801	2.7611	4.7717
$10^{-6} \cdot c$ / K^3	136.9	150.02	135.52
$10^{-6} \cdot d$ / K^3·MPa^{-1}	0.31927	0.43357	0.2067

e / $K^3 \cdot MPa^{-2}$	-161.67	97.933	-140.13
AAD / %	4.3	1.8	2.9
Bias / %	-0.2	0.0	-0.1
MaxD / %	14.4	8.0	9.5

TABLE 4

Pressure-viscosity coefficients, $\alpha(p)$/GPa^{-1}, for the ILs measured in this work.

p / MPa	T / K		
	313.15	343.15	363.15
	$[C_1OC_2C_1Pyrr][(C_2F_5)_3PF_3]$		
0.1	17.0	13.6	12.5
50	16.2	13.0	12.1
150	14.8	12.1	11.3
	$[C_4C_1C_1Im][(C_2F_5)_3PF_3]$		
0.1	17.6	13.8	-
50	17.6	13.8	-
150	17.5	13.8	-
	$[C_4C_1C_1Im][NTf_2]$		
0.1	12.2	9.7	9.3
50	11.5	9.2	8.9
150	10.3	8.4	8.1

TABLE 5

Characteristic parameters (η_0, A_η γ, ϕ) and (η_0^*, A_{η^*} γ^*, ϕ^*) for equations (8) and (9) and average absolute deviations, AAD, of the correlations.

IL	η_0 / mPa·s	A / K·g$^{-\gamma}$·cm$^{3\cdot\gamma}$	γ	ϕ	AAD / %	$10^3\cdot\eta_0^*$	A* / K·g$^{-\gamma^*}$·cm$^{3\cdot\gamma^*}$	γ^*	ϕ^*	AAD / %
$[C_1OC_2C_1Pyrr][(C_2F_5)_3PF_3]$	3.4581	62.4	4.29	2.34	4.6	0.3678	73.4	4.05	2.29	2.9
$[C_1OC_2C_1Pyrr][NTf_2]$	2.6248	131.6	3.38	2.48	4.3	0.3147	147.4	3.16	2.47	3.7
$[C_2C_1Im][C_2SO_4]$	4.0854	241.4	2.69	3.17	5.3	0.5221	254.1	2.52	3.17	5.6
$[C_4C_1Pyrr][NTf_2]$	2.1631	178.7	3.16	2.36	3.9	0.2810	193.2	2.95	2.41	3.3
$[C_4C_1C_1Im][(C_2F_5)_3PF_3]$	3.0338	87.6	3.74	2.57	3.6	0.4328	94.5	3.54	2.70	4.0
$[C_4C_1C_1Im][NTf_2]$	1.9146	196.4	2.73	2.57	2.8	0.2253	214.1	2.57	2.54	2.5

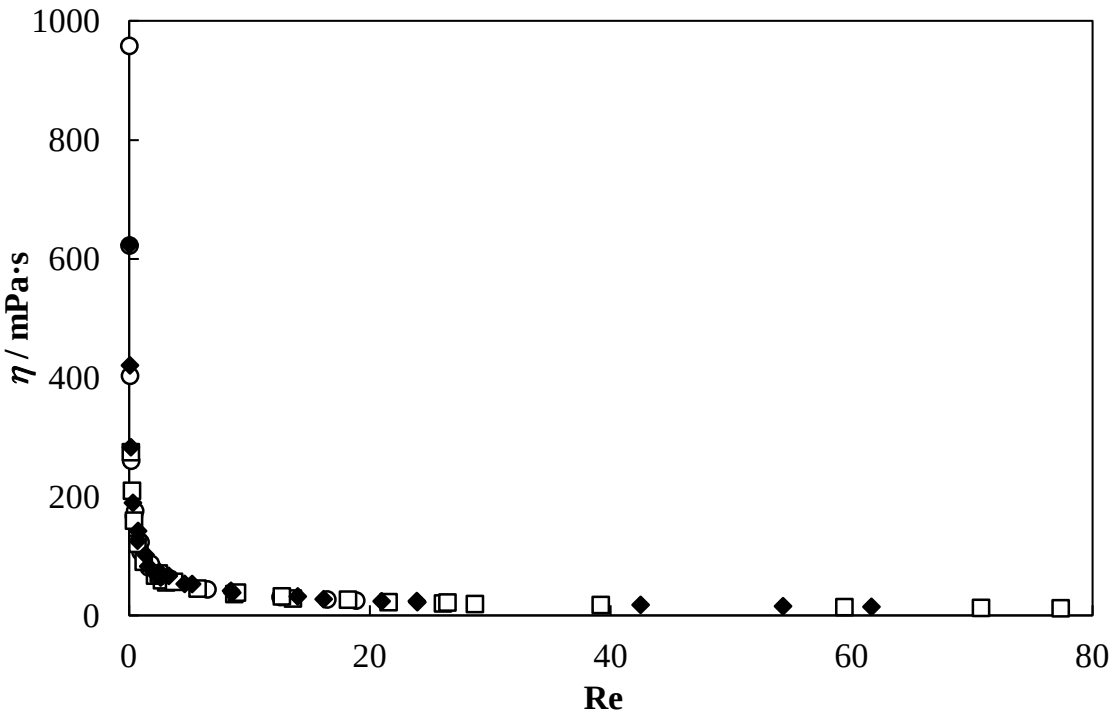

FIGURE 1. Reynolds number according to the Isdale et al. [54] criteria for the fluids under study (Laminar flow Re < 1000). (○) $[C_4C_1C_1Im][(C_2F_5)_3PF_3]$, (◆) $[C_1OC_2C_1Pyrr][(C_2F_5)_3PF_3]$ and (□) $[C_4C_1C_1Im][NTf_2]$.

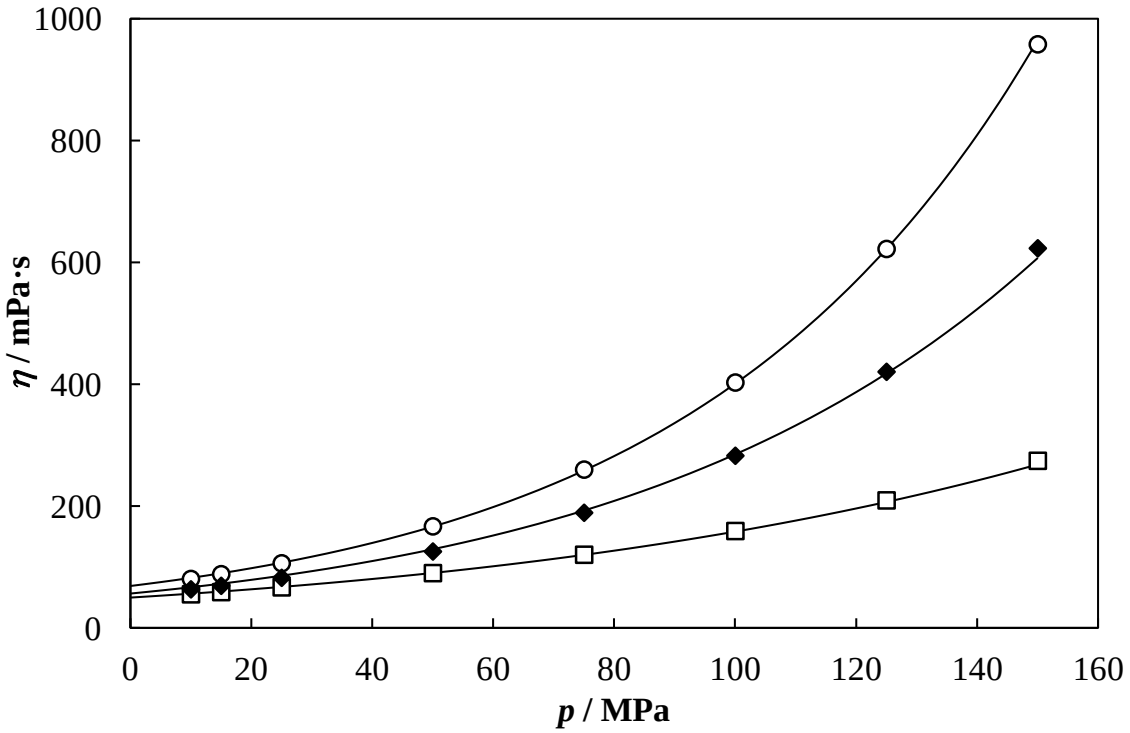

FIGURE 2. Dynamic viscosity at T =313.15 K as a function of the pressure for: (○) $[C_4C_1C_1Im][(C_2F_5)_3PF_3]$, (◆) $[C_1OC_2C_1Pyrr][(C_2F_5)_3PF_3]$ and (□) $[C_4C_1C_1Im][NTf_2]$. The solid lines represent the values obtaining using the equation proposed by Comuñas et al [38] and parameters from table 3.

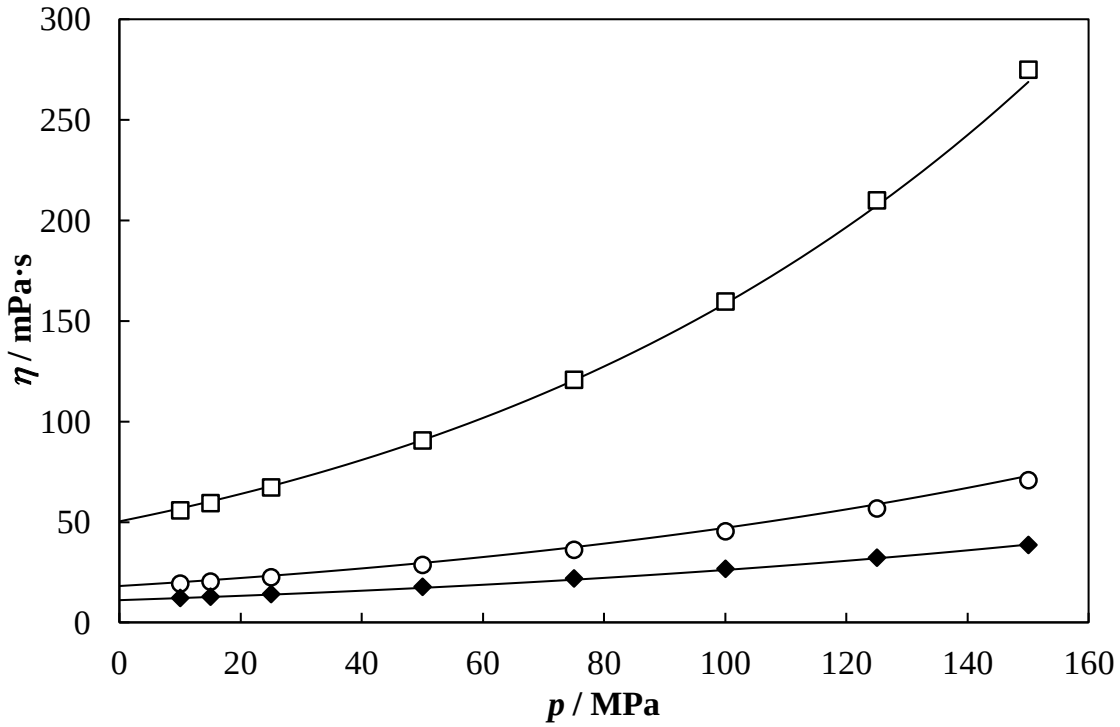

FIGURE 3. Dynamic viscosity of $[C_4C_1C_1Im][NTf_2]$ as a function of the temperature and pressure: (□) 313. 15 K, (○) 343.15 K and (◆) 363.15 K. The solid lines represent the values obtaining using the equation proposed by Comuñas et al [38] and parameters from table 3.

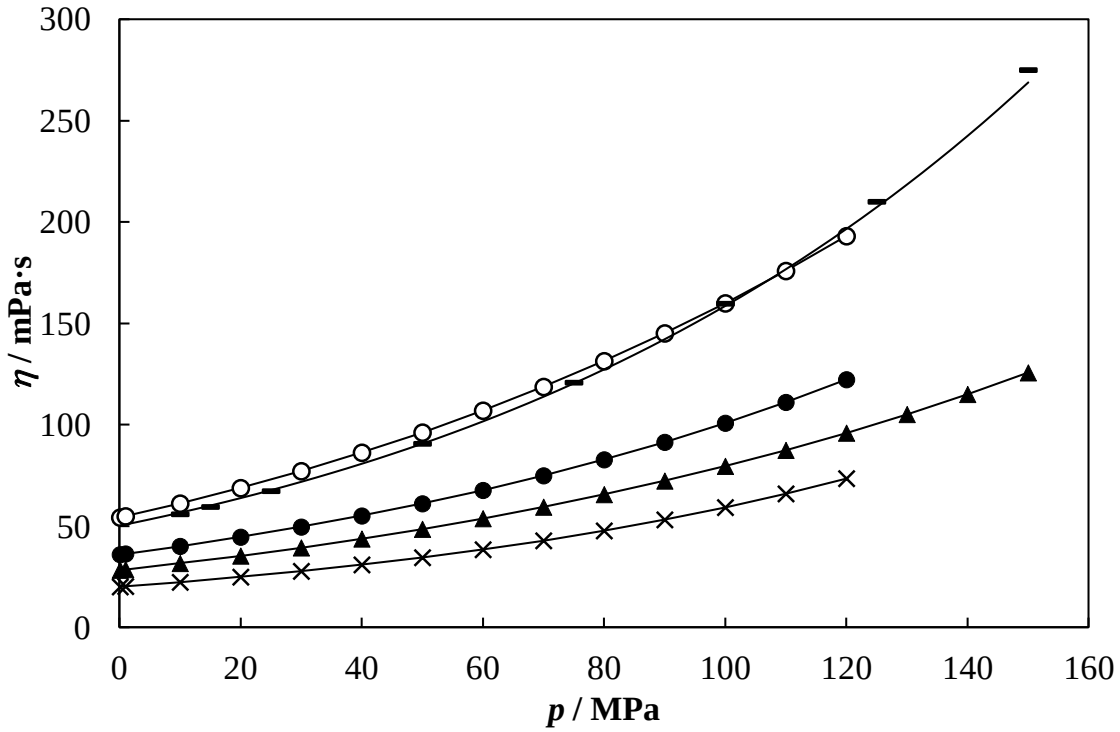

FIGURE 4. Dynamic viscosity at T =313.15 K as a function of the pressure for: (○) $[C_{10}C_1Im][NTf_2]$ [55], (–) $[C_4C_1C_1Im][NTf_2]$ [this work], (●) $[C_6C_1Im][NTf_2]$ [55], (▲) $[C_4C_1Im][NTf_2]$ [24], and (×) $[C_2C_1Im][NTf_2]$ [55].

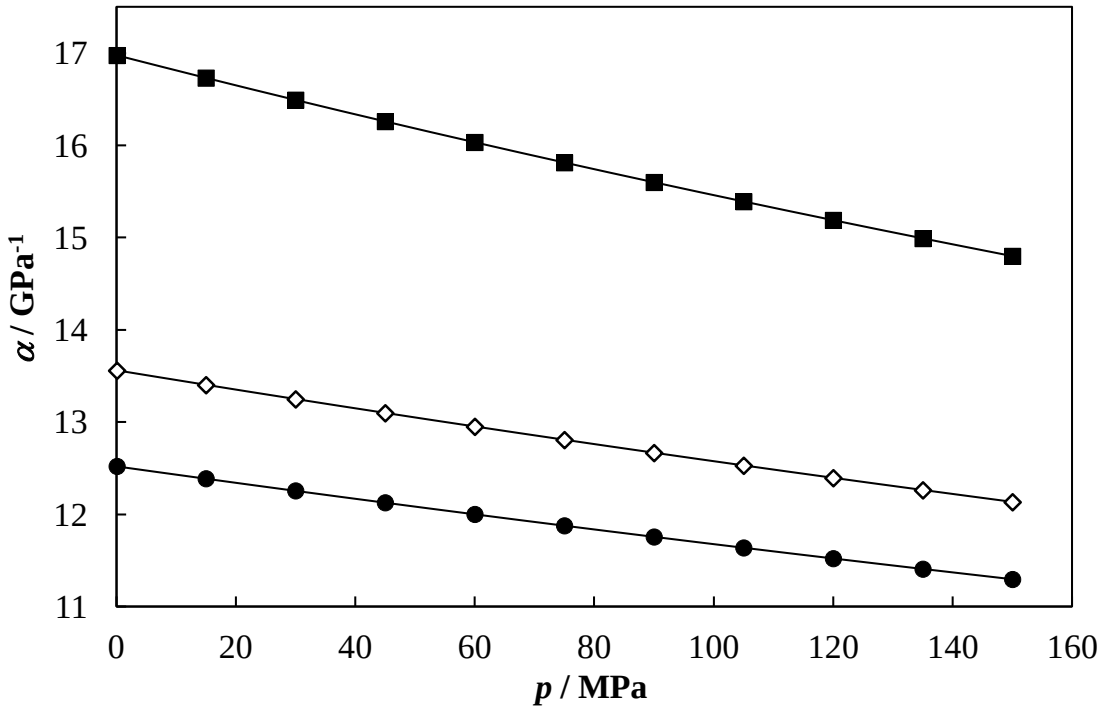

FIGURE 5. Local pressure-viscosity coefficient as a function of pressure for $[C_1OC_2C_1Pyrr][(C_2F_5)_3PF_3]$: (■) 313.15 K, (◇) 343.15 K (●) 363.15 K.

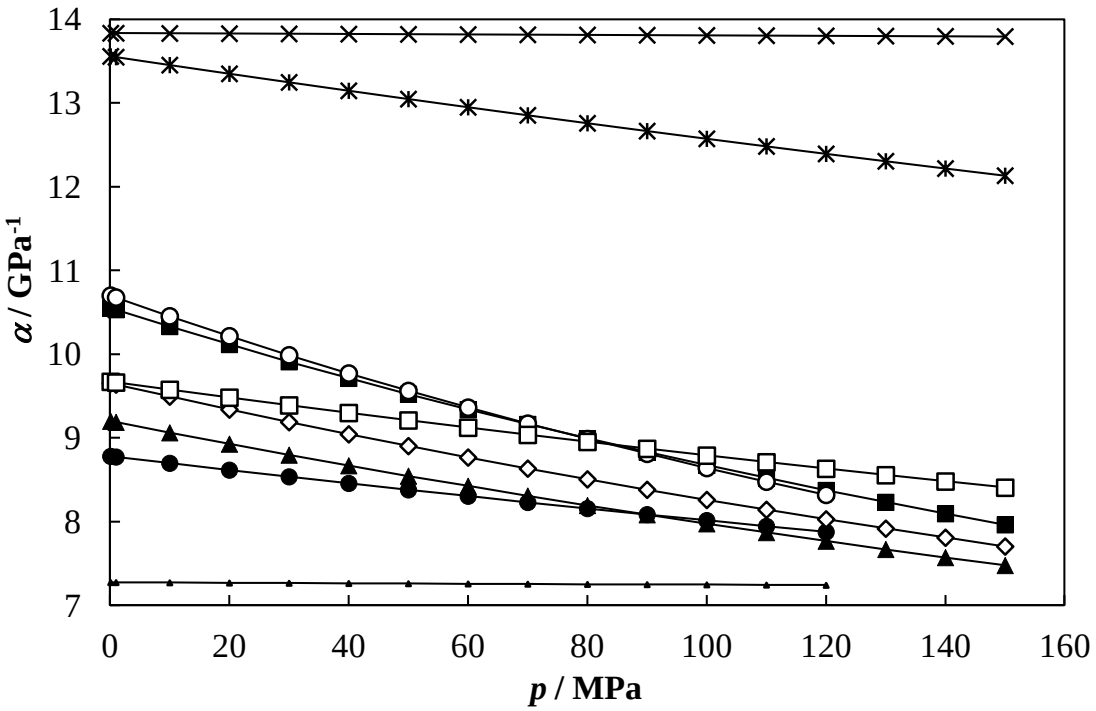

FIGURE 6. Local pressure-viscosity coefficient as a function of pressure at 343.15 K for: (×) $[C_4C_1C_1Im][(C_2F_5)_3PF_3]$, (∗) $[C_1OC_2C_1Pyrr][(C_2F_5)_3PF_3]$, (○) $[C_{10}C_1Im][NTf_2]$[55], (■) $[C_4C_1Pyrr][NTf_2]$[22], (□) $[C_4C_1C_1Im][NTf_2]$, (◆) $[C_1OC_2C_1Pyrr][NTf_2]$, (▲) $[C_4C_1Im][NTf_2]$[24], (●) $[C_6C_1Im][NTf_2]$[55], (△) $[C_2C_1Im][NTf_2]$[55].

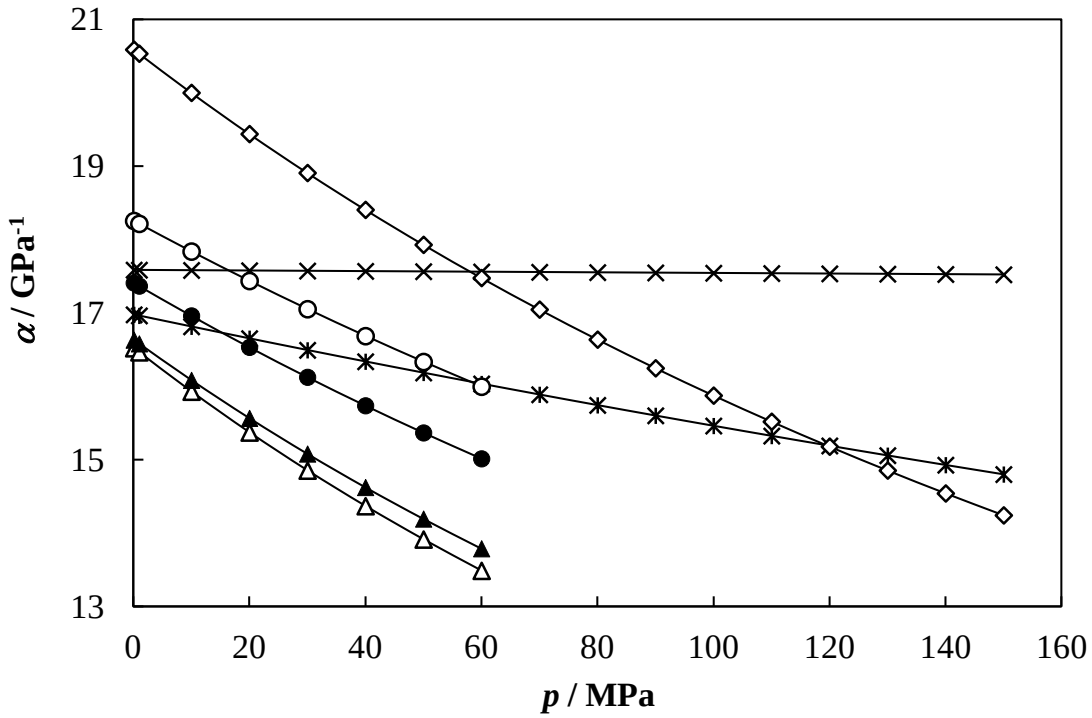

FIGURE 7. Local pressure-viscosity coefficient as a function of pressure at 313.15 K for: (◇) squalane [47], (○) PAG3 [17], (×) $[C_4C_1C_1Im][(C_2F_5)_3PF_3]$ [this work], (●) PAG2 [44], (∗) $[C_1OC_2C_1Pyrr][(C_2F_5)_3PF_3]$ [this work], (▲) dipentaerythritol heptanoate [43], and (△) dipentaerythritol pentanoate [43].

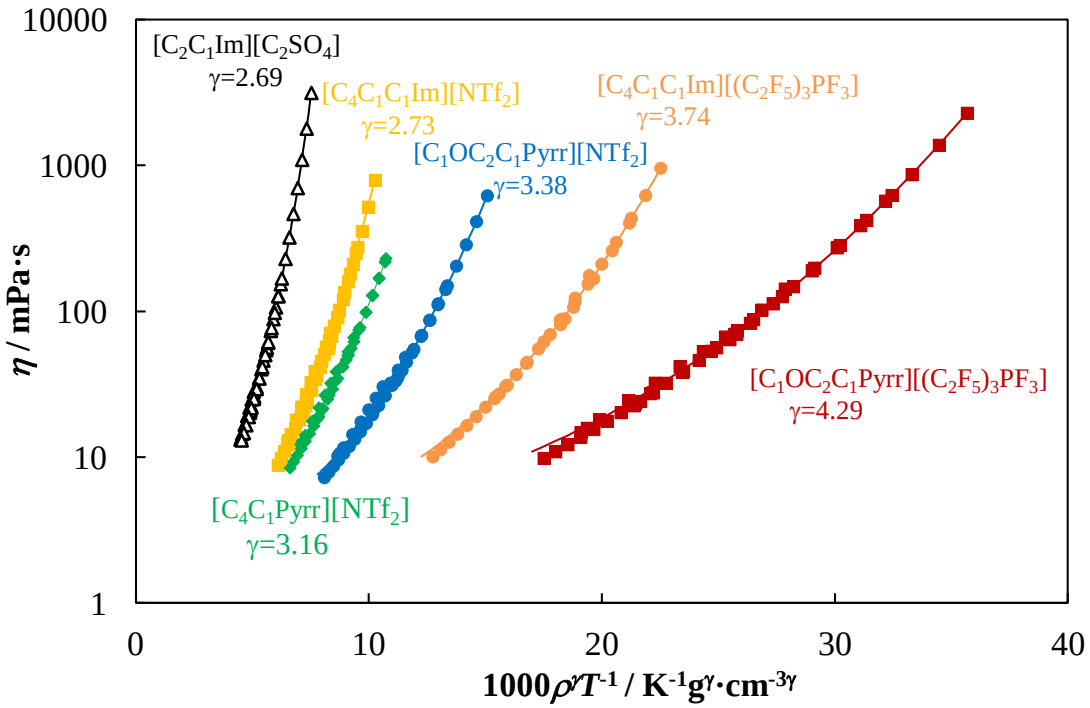

FIGURE 8. Superposition of the viscosity η of the ILs studied by fitting the γ values to the experimental data. The solid lines are the fits of equation (8).

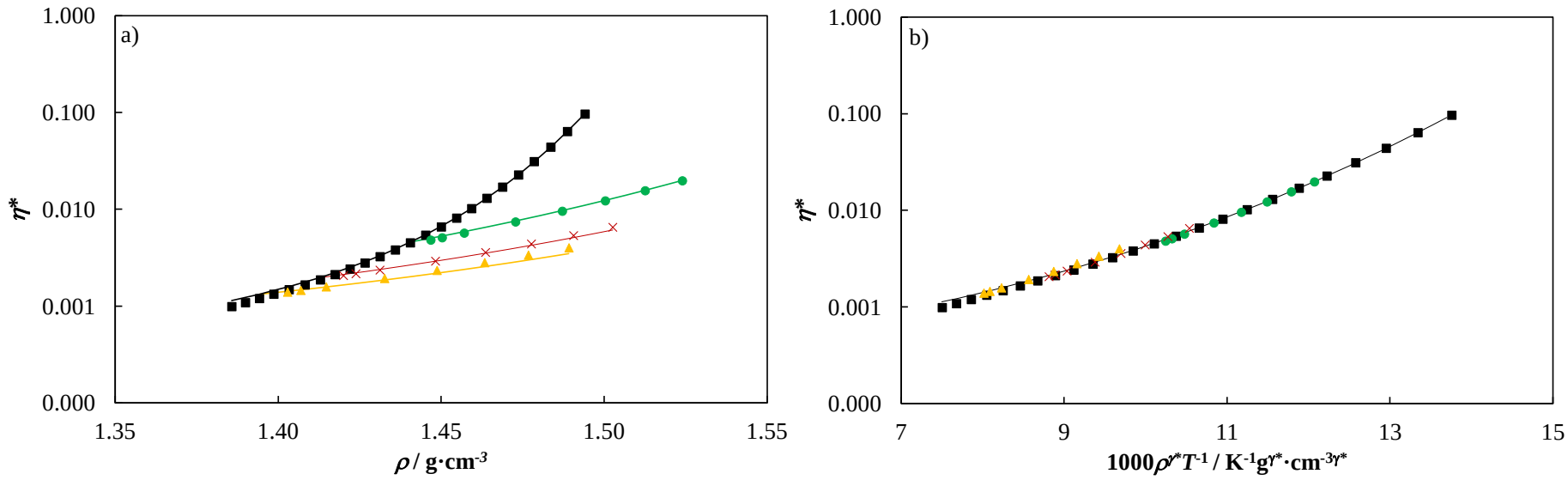

FIGURE 9. Reduced viscosity of $[C_1OC_2C_1Pyrr][NTf_2]$ a) against density; b) against the function $1000\rho^{\gamma^*}\cdot T^{-1}$. The solid lines are the fit of equation (8). (■) 0.1 MPa, (●) 313.15 K, (×) 343.15 K, (▲) 363.15K.